

INFLUENCE OF PRESSURE AND ATOMIC CONCENTRATION ON STRUCTURE AND MECHANICAL PROPERTIES OF CuNi ALLOY BY MOLECULAR DYNAMICS SIMULATION

Nguyen Thi Thao and Trinh Thi Thu Hang

Faculty of Physics, Hanoi National University of Education

Abstract. The structure and mechanical properties of $\text{Cu}_{80}\text{Ni}_{20}$ and $\text{Cu}_{50}\text{Ni}_{50}$ alloys with the size of 4000 atoms have been investigated using molecular dynamic (MD) simulation. The interactions between atoms of the system were calculated by the Sutton-Chen type of embedded atom method. Using a cooling rate of 0.01 K/ps, we find that both Ni and Cu atoms are crystallized into face centered cubic (fcc) and the hexagonal close packed (hcp) phases when the sample was cooled down to 300 K. The atomic concentration of CuNi alloy samples have a different effect on this crystallization. The transformation to the crystalline phase is analyzed through the Common Neighbor Analysis (CNA) methods. Furthermore, we focus on the dependence of the mechanical properties of CuNi alloy on pressure and atomic concentration.

Keywords: molecular dynamics, CuNi alloy, CNA method, structure, mechanical properties.

1. Introduction

Due to many industrial applications, Cu-Ni alloys are widely studied in the world. Compared to pure Cu, Cu-Ni alloys are better in electrical resistance, durability, rigidity, thermoelectric properties, resistance to corrosion, and ease of fabrication [1]. The addition of nickel to copper helps improve durability and resistance to corrosion while allowing the alloy to remain flexible. Depend on the cooling rate, different types of Cu-Ni alloys are formed during the cooling process. Numerous studies have shown glass transition, crystallization of Cu-Ni amorphous alloys during heat treatment, liquid Cu-Ni alloys during cooling, and dependence pressure of processes [2-4]. The results indicate that the glass transition temperature and the crystal transition temperature of Cu-Ni alloys increase as the pressure increases. The corrosive properties and biochemical reactions of $\text{Cu}_{90}\text{Ni}_{10}$ and $\text{Cu}_{70}\text{Ni}_{30}$ alloys (corresponding to Ni concentrations of 10% and 30%) in seawater studied show that these alloys have good

Received February 26, 2020. Revised June 18, 2020. Accepted June 25, 2020.

Contact Nguyen Thi Thao, e-mail address: thaont@hnue.edu.vn

corrosion resistance. Many studies on Fe-Cu-Ni containing materials have been conducted [5-6]. With the simulation method, dynamic Monte Carlo simulation and molecular dynamics simulation were used to simulate the structural characteristics of Cu-rich clusters in α -Fe with different pore concentrations [7]. The influence of the size of Cu precipitates on the mechanical properties of steel was studied by Finite Element Method [8]. The results indicated that the strength of the matrix (strength of matrix) first increased then decreased with the increasing size of Cu-rich clusters. Cu content affects the structural and mechanical changes of these alloys. However, the mechanism of influence of Cu content on the structural and mechanical properties of CuNi alloy at different pressures has not been clarified. Therefore, the research focuses on the structural and mechanical properties of CuNi alloys with different atomic concentration and pressure.

2. Content

2.1. Computational procedures

An MD simulation was conducted to study CuNi alloys. We use the Sutton-Chen type of embedded atom method to describe the inter-atomic potential between atoms [3]. This potential was widely used for investigating the metallic systems and their alloys. It has also been used in the investigations of liquid and amorphous phases [9]. The MD simulation is performed for samples of $\text{Cu}_{80}\text{Ni}_{20}$ and $\text{Cu}_{50}\text{Ni}_{50}$ (corresponding to Cu concentrations of 80% and 50%) containing 4000 particles under periodic boundary conditions. These samples were first heated to 2000 K to break the initial random state. These samples then were cooled to 300 K with a cooling rate of 0.01 K/ps to study their crystallization. In this way, eight CuNi alloy samples which contain 3200 Cu and 800 Ni atoms have been constructed at eight different pressure from 0GPa to 45GPa. The procedure is the same for CuNi alloy samples which contain 2000 Cu and 2000 Ni atoms. The transformation to the crystalline phase is analyzed through the Common Neighbor Analysis (CNA) methods [10]. The structural transformation to the crystalline phase is analyzed through the radial distribution function (RDF). It is defined as:

$$g(r) = \frac{V}{N^2} \left[\frac{\sum_i n_i(r)}{4\pi r^2 \Delta r} \right]$$

here, r is the radial distance, $n_i(r)$ is the coordination number of atoms separated with r within Δr interval, and brackets denote the time average [4].

The mechanical properties of CuNi alloys determined by the deformation of the sample on an axis.

2.2. Results and discussion

The phase transition from liquid to solid can be performed via the change of the potential energy (PE) of the system. Figure 1 shows the change of the PE of $\text{Cu}_{80}\text{Ni}_{20}$ and $\text{Cu}_{50}\text{Ni}_{50}$ samples at 45 GPa during cooling processes. The results indicate that there are drastic drops of the potential energy, which means that atoms transfer from disordered structure of liquid to ordered structure of the crystal. So, the crystallization has happened during the cooling processes. The potential energy of $\text{Cu}_{80}\text{Ni}_{20}$ samples

drops drastically corresponding to the temperature down from $T_1 = 1150$ K to $T_2 = 950$ K. This temperature range is less than that (1200 K - 1050 K) of $\text{Cu}_{50}\text{Ni}_{50}$ samples due to the effect of concentration atoms.

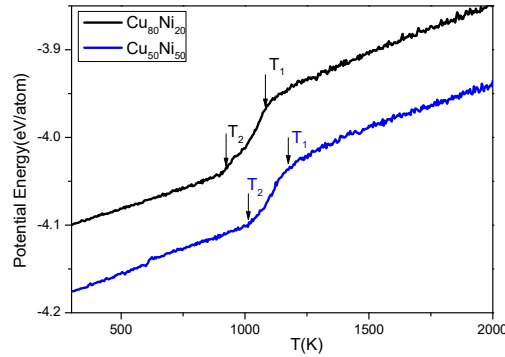


Figure 1. Dependence on the temperature of potential energy under the cooling process at the pressure of 45 GPa

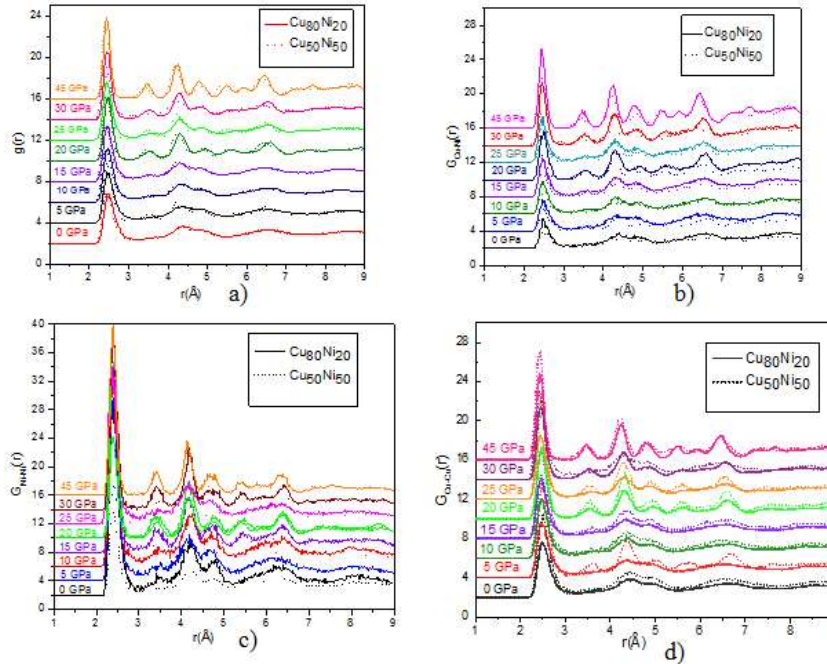


Figure 2. The RDF of $\text{Cu}_{80}\text{Ni}_{20}$ and $\text{Cu}_{50}\text{Ni}_{50}$ samples at 300 K
 a) The total radial distribution function $G(r)$ of CuNi samples;
 b) The pair RDF $G_{\text{Cu-Ni}}(r)$ for Cu-Ni pair; c) The pair RDF $G_{\text{Cu-Cu}}(r)$ for Cu-Cu pair;
 d) The pair RDF $G_{\text{Ni-Ni}}(r)$ for Ni-Ni pair

Figure 2 displays the total RDFs for $G(r)$ and pair RDFs of $\text{Cu}_{80}\text{Ni}_{20}$ and $\text{Cu}_{50}\text{Ni}_{50}$ samples at 300 K. For the total RDFs $G(r)$ exhibiting the short-order structure of amorphous phase at 0 GPa for both $\text{Cu}_{80}\text{Ni}_{20}$ and $\text{Cu}_{50}\text{Ni}_{50}$ samples (see Figure 2a). We can see that the agreement of the position of the first peak, which is located at 2.48 Å. The model structure is in the amorphous phase for pressure less than 20 GPa at the

300 K temperature. With increasing pressure, the total RDFs of $\text{Cu}_{80}\text{Ni}_{20}$ and $\text{Cu}_{50}\text{Ni}_{50}$ samples show a crystalline structure at 45 GPa. For the $G_{\text{Cu-Ni}}(r)$ exhibiting the Cu-Ni bond distance (see Figure 2b), the position of the first peak is unchanged with increasing pressure, the height of the first peak increases with increasing pressure. For the $G_{\text{Ni-Ni}}(r)$ exhibiting the Ni-Ni bond distance (see Figure 2c), $G_{\text{Ni-Ni}}(r)$ is complexly dependent on pressure and concentration of atoms. For the $G_{\text{Cu-Cu}}(r)$ exhibiting the Cu-Cu bond distance (see Figure 2d), the shape of RDFs is different for $\text{Cu}_{80}\text{Ni}_{20}$ and $\text{Cu}_{50}\text{Ni}_{50}$ samples at pressures of 5 GPa; 15 GPa and 30 GPa.

For a detailed explanation of the structure of these samples, we used the common neighbor analysis (CNA) method. With the CNA method, we indicated the total number of crystal atom of $\text{Cu}_{80}\text{Ni}_{20}$ and $\text{Cu}_{50}\text{Ni}_{50}$ alloy samples. The crystal atoms containing both faced centered cubic or hexagonal closed packed structures at 300 K.

The pressure dependence of the total number of crystal atoms of $\text{Cu}_{80}\text{Ni}_{20}$ and $\text{Cu}_{50}\text{Ni}_{50}$ alloy samples are listed in Table 1. When the pressure increasing, the total number of crystal atoms is complex transformations. At pressures of 5 GPa; 15 GPa and 30 GPa, the total number of crystal atoms have a great difference for $\text{Cu}_{80}\text{Ni}_{20}$ and $\text{Cu}_{50}\text{Ni}_{50}$ alloy samples. At a pressure of 45 GPa, the crystallization of Cu-Ni alloy sample is almost complete with 97% and 99.7% number of crystal atoms for $\text{Cu}_{80}\text{Ni}_{20}$ and $\text{Cu}_{50}\text{Ni}_{50}$ alloy samples, respectively.

Table 1. Pressure dependence of the Total number of crystal atoms of $\text{Cu}_{80}\text{Ni}_{20}$ and $\text{Cu}_{50}\text{Ni}_{50}$ alloy samples

Pressure (GPa) \ Samples	0	5	10	15	20	25	30	45
$\text{Cu}_{80}\text{Ni}_{20}$	2298	1612	2231	2028	3328	3447	3627	3882
$\text{Cu}_{50}\text{Ni}_{50}$	2471	3693	2780	3400	3970	3874	2913	3989

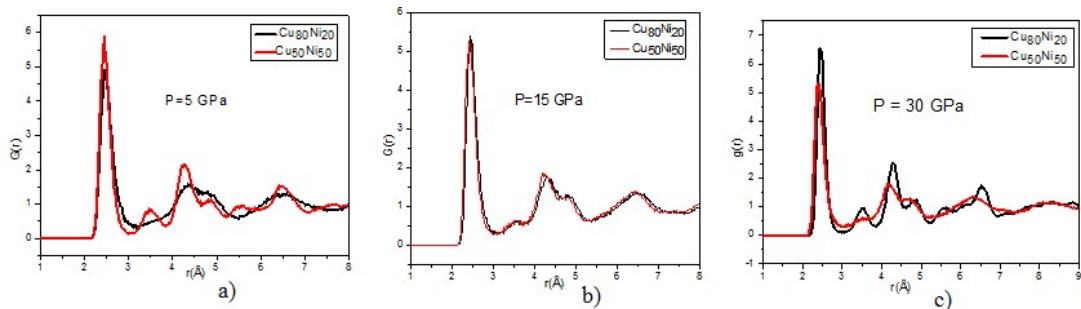


Figure 3. The total radial distribution function $G(r)$ of $\text{Cu}_{80}\text{Ni}_{20}$ and $\text{Cu}_{50}\text{Ni}_{50}$ alloy samples at 300 K: a) $G(r)$ at a pressure of 5 GPa; b) $G(r)$ at a pressure of 15 GPa; c) $G(r)$ at a pressure of 30 GPa

The above results show the complex dependence of the structure of the samples on the pressure and atomic concentration, especially at a pressure of 5 GPa, 15 GPa and 30 GPa. Therefore, we show the total radial distribution function of $\text{Cu}_{80}\text{Ni}_{20}$ and $\text{Cu}_{50}\text{Ni}_{50}$ alloy samples at this pressure to clarify this difference. Figure 3 displays the total radial distribution function $G(r)$ of $\text{Cu}_{80}\text{Ni}_{20}$ and $\text{Cu}_{50}\text{Ni}_{50}$ alloy samples at a pressure of 5 GPa, 15 GPa and 30 GPa at 300 K. At a pressure of 5 GPa, $G(r)$ of $\text{Cu}_{50}\text{Ni}_{50}$ alloy sample shows the crystal phase in accordance with the number of crystal atoms of 3693 atoms. This phenomenon also occurs at a pressure of 30 GPa for $\text{Cu}_{80}\text{Ni}_{20}$ sample with the number of crystal atoms of 3627 atoms.

The crystallization of $\text{Cu}_{80}\text{Ni}_{20}$ and $\text{Cu}_{50}\text{Ni}_{50}$ alloy samples can be seen from the snapshot of the spatial arrangement of atoms. As shown in Figure 4, a crystal structure forms inside the samples and then grows with increasing pressure for $\text{Cu}_{80}\text{Ni}_{20}$ samples. As the number of crystal-atoms increases from 1612 atoms at a pressure of 5 GPa to 3882 atoms at a pressure of 45 GPa (see Figures 4a, 4b, 4c). For $\text{Cu}_{50}\text{Ni}_{50}$ samples, the crystal structure is shown most clearly at 5 GPa with the number of crystal atoms of 3693 atoms, and it decreases to 2913 atoms at a pressure of 30 GPa (see Figures 4d, 4e, 4f).

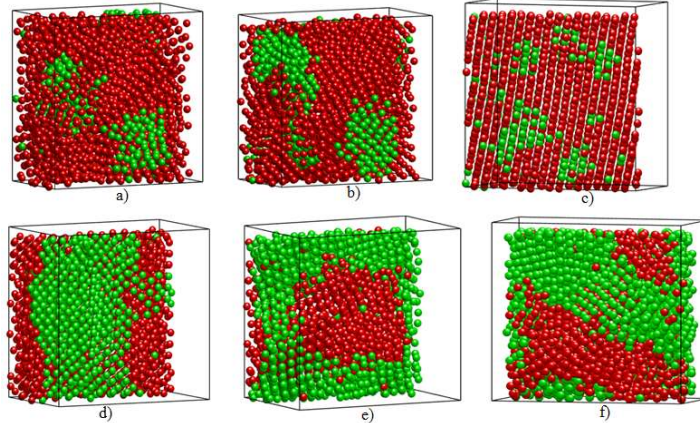


Figure 4. The snapshot atoms of $\text{Cu}_{80}\text{Ni}_{20}$ and $\text{Cu}_{50}\text{Ni}_{50}$ alloy samples under compression: Figures a), b), c) are snapshots of $\text{Cu}_{80}\text{Ni}_{20}$ samples at 5, 15, 30 GPa, respectively; Figures d), e), f) are snapshots of $\text{Cu}_{50}\text{Ni}_{50}$ samples at 5, 15, 30 GPa, respectively

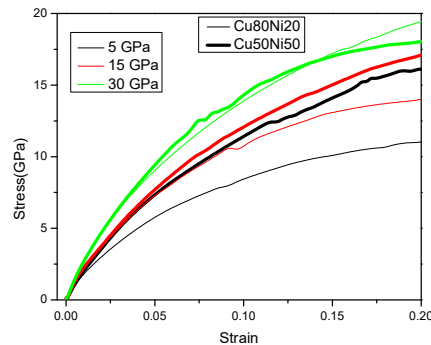


Figure 5. Stress-strain curves for $\text{Cu}_{80}\text{Ni}_{20}$ and $\text{Cu}_{50}\text{Ni}_{50}$ alloy samples upon compression at a pressure of 5GPa, 15GPa and 30 GPa

Here we also showed the mechanical properties of Cu₈₀Ni₂₀ and Cu₅₀Ni₅₀ alloy samples upon compression. We calculated the stress as a function of uniaxial strain during deformation of the samples. The stress-strain curves in samples at different pressure obtained from the MD simulation are presented in Figure 5. The elastic modulus is given by the slope of the stress-strain curve in the linear region. From the stress-strain curves, we intimated the elastic modulus of the samples as presented in Table 2. The elastic modulus increases with increasing pressure (from 135.6 GPa at a pressure of 0 GPa to 263.4 GPa at a pressure of 45 GPa) for Cu₈₀Ni₂₀ alloy samples, and this result is in good agreement with one in Ref. [11]. For Cu₅₀Ni₅₀ alloy samples, the elastic modulus increases with increasing pressure without the pressure of 20 GPa. At a pressure of 20 GPa, the elastic modulus is 144.3 GPa.

Table 2. Pressure dependence of the elastic modulus of Cu₈₀Ni₂₀ and Cu₅₀Ni₅₀ alloy samples

Pressure (Gpa) E (GPa)	0	5	10	15	20	25	30	45
Cu ₈₀ Ni ₂₀	135.6	143.1	149.2	150.6	165.9	185.2	205.5	263.4
Cu ₅₀ Ni ₅₀	129.3	144.6	152.9	161.6	144.3	195.4	211.1	235.8

3. Conclusions

The structural transform of CuNi sample has been studied by molecular dynamics simulations upon the cooling process at different pressures. The phase transition was observed in the temperature range between T₁ = 1150 K and T₂ = 950 K for Cu₈₀Ni₂₀ samples; T₁ = 1200 K and T₂ = 1050 K for Cu₅₀Ni₅₀ samples. The structural transformation to the crystalline phase is analyzed through the radial distribution function and the common neighbor analysis method. The result shows that both Ni and Cu atoms are crystallized into face centered cubic and the hexagonal close packed phases. CuNi samples exhibit both elastic and plastic deformations under the uniaxial tension test. The elastic modulus increases with increasing pressure for Cu₈₀Ni₂₀ alloy samples.

Acknowledgements. This work is supported by the Vietnam Ministry of Education and Training under Grant Number B2020-SPH-01.

REFERENCES

- [1] M. Hennes, J. Buchwald and S. G. Mayr, 2012. Structural properties of spherical Cu/Ni nanoparticles. *Cryst. Eng. Comm.*, 14, 7633.
- [2] F.A. Celik, 2013. Cooling rate dependence of the icosahedral order of amorphous CuNi alloy: A molecular dynamics simulation. *Vacuum*, 97, 30.

- [3] S.Kazanc, 2007. Molecular dynamics study of pressure effect on crystallization behaviour of amorphous CuNi alloy during isothermal annealing. *Physics Letters A*, Volume 365, Issues 5-6, pp. 473-477.
- [4] S.Kazanc, 2006. Molecular dynamics simulations of pressure effect on glass formation and the crystallization in liquid CuNi alloy. *Computational Materials Science*, 38, pp. 405-409.
- [5] N. Gao, K.F. Wei, S.X. Zhang, Z.G. Wan, 2012. The Energy State and Phase Transition of Cu Clusters in bcc-Fe Studied by a Molecular Dynamics Simulation. *Chin. Phys. Lett.* 29, 096102.
- [6] J.J. Blackstock, G.J. Ackland, 2001. Phase transitions of copper precipitates in Fe-Cu alloys. *Philos. Mag. A* 81, pp. 2127-2148.
- [7] D. Molnar, R. Mukherjee, A. Choudhury, A. Mora, 2012. Multiscale simulations on the coarsening of Cu-rich precipitates in α -Fe using kinetic Monte Carlo, molecular dynamics and phase-field simulations. *Acta Mater.* 60, pp. 6961-6971.
- [8] L.J. Hu, S.J. Zhao, Q.D. Liu, 2012. Effect of environment on fatigue strength of Cu/Si interface in nanoscale components. *Mater. Sci. Eng., A* 556, pp. 140-146.
- [9] J.H.Shim, S.C.Lee, B.J.Lee, J.Y.Suh, Y.W.Cho, 2003. Molecular dynamics simulation of the crystallization of a liquid gold nanoparticle. *J. Cryst.Growth*, 250, pp. 558-564.
- [10] Helio Tsuzuki, Paulo S. Branicio Jose P Rino, 2007. Structural characterization of deformed crystal by analysis of common atomic neighborhood. *Computer Physics Communications*, 177, pp. 518-523.
- [11] Giang T. Nguyen, Thao T. Nguyen, Trang T. Nguyen, Vinh V. Le, 2016. Molecular dynamics simulations of pressure-induced structural and mechanical property changes in amorphous Al₂O₃. *Journal of Non-Crystalline Solids*, 449, pp. 100-106.